Kerr Nonlinearity via Cascaded Optical Rectification and the Linear Electro-optic Effect

Ch. Bosshard, R. Spreiter, M. Zgonik, and P. Günter
Nonlinear Optics Laboratory, Institute of Quantum Electronics, ETH Hönggerberg, CH-8093 Zürich, Switzerland
(Received 28 November 1994)

We show both theoretically and experimentally that the combined processes of optical rectification and the linear electro-optic effect lead to an effective nonlinear refractive index n_2 in noncentrosymmetric materials. This cascaded second-order nonlinear optical effect arises in addition to the well-known contribution due to second-harmonic generation and difference-frequency mixing and is of comparable magnitude. However, it has the advantage of a broad acceptance angle because no precise phase matching is needed. Experimental results in $KNbO_3$ crystals are presented.

PACS numbers: 78.20.Jq, 42.65.Ky, 42.65.Pc, 42.70.Nq

Large, nonresonant optical Kerr-like nonlinearities are a basic requirement for all-optical switching and related applications [1]. Besides the third-order nonlinear susceptibility $\chi^{(3)}$, symmetry allowed in all materials, there is another important contribution that occurs only in noncentrosymmetric media. This contribution leads to a nonlinear phase shift of the interacting waves in nearly phase-matched second-harmonic generation and other parametric processes [2,3]. Such effects were first observed in high-power pulsed second-harmonic generation experiments [2,3].

Some years ago the potential of increasing the magnitude of a third-order nonlinear effect with a combination of cascaded second-order effects was discovered and demonstrated using a nonlinear transmission line resonator [4]. Recently the potential for all-optical switching was realized [5,6] and large nonlinear phase shifts due to cascading were observed for the first time in potassium titanyl phosphate (KTP) waveguides [7]. Unexpectedly large nonlinear refractive index changes observed in fibers of 4-(N,N-dimethylamino)-3-acetamidonitrobenzene (DAN) could also be explained by cascaded nonlinearities [8].

We now demonstrate, for the first time to our knowledge, that the combined processes of optical rectification and the linear electro-optic effect give rise to a large effective nonlinear refractive index n_2, which is defined as $n = n_0 + n_2 I$, where n_0 is the linear refractive index and I is the intensity of the incoming beam. This combined effect was already observed in four-wave mixing experiments with picosecond lasers in $KNbO_3$ [9] and identified in self-modulation of picosecond pulses in GaAs [10]. Here we present a quantitative analysis taking into account all three contributions (direct $\chi^{(3)}$, second-harmonic generation, optical rectification and electro-optics). In addition we present the first experimental evidence of this new contribution to n_2 in $KNbO_3$ crystals. In order to analyze the results obtained in polar $KNbO_3$ we also did similar experiments in cubic $KTaO_3$, where only the direct third-order processes are allowed by symmetry.

In this work the total polarization P in a medium induced by an incident electric field is given by

$$P_i(t) = \varepsilon_0(\chi^{(1)}_{ij} E_j + \chi^{(2)}_{ijk} E_j E_k + \chi^{(3)}_{ijkl} E_j E_k E_l + \cdots), \tag{1}$$

assuming summation over common indices, and where $\chi^{(n)}$ describes the nonlinear optical susceptibility of n^{th} order. The electric field of the incident wave is defined as

$$E_i(t) = \tfrac{1}{2}(E_i e^{-i\omega t} + E_i^* e^{i\omega t}). \tag{2}$$

In centrosymmetric media the third-order susceptibility $\chi^{(3)}$ is the dominant contribution to the nonlinear refractive index n_2. The relation between $\chi^{(3)}$ and n_2 can be deduced from Eq. (1) and is given by [10]

$$n_2 = \frac{3\chi^{(3)}}{4c\varepsilon_0 n_0^2}, \tag{3}$$

where c is the speed of light in vacuum and ε_0 is the vacuum permittivity.

In noncentrosymmetric materials so-called second-order cascaded processes due to second-harmonic generation (SHG) of the incident wave and difference-frequency mixing of the generated second-harmonic wave with the incident wave can lead to an effective nonlinear phase shift. In the undepleted wave approximation this phase shift is proportional to the input intensity and one can write [11]

$$n_2^{\mathrm{SHG}} = -\frac{4\pi}{c\varepsilon_0}\left(\frac{L}{\lambda_0}\right)\frac{d_{\mathrm{eff}}^2}{n^{2\omega}(n^{\omega})^2}\,\frac{1}{\Delta kL}, \tag{4}$$

where n_2^{SHG} is the contribution to n_2 from this type of interaction, λ_0 is the wavelength of the fundamental in vacuum, d_{eff} is the effective nonlinear optical coefficient ($= \chi_{\mathrm{eff}}/2$), $\Delta k = k^{2\omega} - 2k^{\omega}$ is the phase mismatch, and $k^{\omega} = 2\pi n^{\omega}/\lambda_0$ is the wave vector in the medium. The sign of n_2^{SHG} depends on the sign of the phase-mismatch Δk with n_2^{SHG} being negative for $n^{2\omega} > n^{\omega}$. Far from phase matching n_2^{SHG} is small but always present for $d_{\mathrm{eff}} \neq 0$. Note that for large phase shifts in a nearly phase-matched interaction large depletion of the fundamental beam is required [7,11].

 0031-9007/95/74(14)/2816(4)$06.00

We now introduce an additional contribution to n_2 that has been overlooked previously. In noncentrosymmetric materials an input beam at frequency ω can also generate a quasistatic electric field at frequency zero (optical rectification) and therefore induce a polarization

$$P_i^0 = \tfrac{1}{2}\,\varepsilon_0 \chi_{ijk}^{(0;\omega,-\omega)} E_j^{\omega} E_k^{\omega *}, \tag{5}$$

where $\chi_{ijk}^{(0;\omega,-\omega)}$ is the nonlinear optical susceptibility describing optical rectification [12]. This generated field can induce a refractive index change via the linear electro-optic effect. In the main axis system of the optical indicatrix the linear electro-optic coefficient r_{ijk} itself is defined through

$$\Delta\left(\frac{1}{n^2}\right)_{ij} = r_{ijk} E_k^0 = -\frac{2}{n_i^2 n_j^2} \chi_{ijk}^{(-\omega;\omega,0)} E_k^0, \tag{6}$$

where $\Delta(1/n^2)$ describes the field-induced changes of the optical indicatrix due to a static applied electric field E_k^0. Figure 1 shows a schematic drawing of the principle. For light polarized along a main axis of the optical indicatrix and a refractive index change along the same direction we obtain for the new contribution to the nonlinear refractive index n_2

$$(n_2)_i^{\mathrm{OR}} = \frac{1}{c\varepsilon_0 n_i^2} \frac{\chi_{iik}^{(-\omega;\omega,0)} \chi_{kii}^{(0;\omega,-\omega)}}{(\varepsilon_{kk} - 1)}, \tag{7}$$

where ε_{kk} is the static dielectric constant. By permutation of indices and optical frequencies in $\chi_{ijk}^{(0;\omega,-\omega)}$ we obtain $\chi_{ijk}^{(0;\omega,-\omega)} = \chi_{kji}^{(-\omega;\omega,0)}$ and

$$(n_2)_i^{\mathrm{OR}} = \frac{1}{c\varepsilon_0 n_i^2} \frac{(\chi_{iik}^{(-\omega;\omega,0)})^2}{(\varepsilon_{kk} - 1)} = \frac{n_i^6}{4c\varepsilon_0} \frac{(r_{iik})^2}{(\varepsilon_{kk} - 1)}. \tag{8}$$

We can illustrate the combined processes of optical rectification and the linear electro-optic effect with the following example. We illuminate a plate of a polar crystal with light polarized parallel to the polar axis. The effect of optical rectification will produce a quasistatic field along the polar direction. This field can then act on the beam through a refractive index change produced by the linear electro-optic effect. Obviously, a contribution from second-harmonic generation will also occur at the same time. If we illuminate a plate of a polar crystal with light polarized perpendicular to the polar axis, n_2^{OR} will also be present, e.g., for light propagation along the polar axis, in which case the longitudinal electro-optic effect becomes active. This is in contrast to second-harmonic generation for which the appearance of n_2^{SHG} depends on

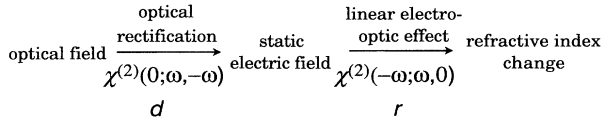

FIG. 1. Process of cascaded second-order effects because of optical rectification and the linear electro-optic effect leading to a Kerr nonlinearity.

the propagation direction. Note that the new contribution n_2^{OR} to the nonlinear refractive index is always phase matched since all interacting waves have either the same optical frequency or have frequency zero.

The nonlinear refractive index n_2 of a noncentrosymmetric material is therefore in general given by

$$n_2 = n_2^{\mathrm{direct}} + n_2^{\mathrm{SHG}} + n_2^{\mathrm{OR}}, \tag{9}$$

where n_2^{direct} is the contribution from direct $\chi^{(3)}$ processes of polar and nonpolar materials. In the following we describe measurements that were carried out with polar $KNbO_3$ (point group $mm2$) and nonpolar $KTaO_3$ (point group $m3m$) to experimentally verify Eq. (9).

The measurements were done with the Z-scan technique [13]. The technique requires only a single focused beam and a circular aperture placed in the far field behind the sample. The sample is translated along the optical axis through the focused laser beam. This translation leads to a change of the incident intensity and therefore to a variable refractive index change induced by n_2. Measuring the transmission through the circular aperture after the sample the sign as well as the magnitude of n_2 can be determined [13]. A performance of the same experiment without the aperture allows the determination of the two-photon absorption α_2 (defined through $\alpha = \alpha_0 + \alpha_2 I$, where α_0 is the linear absorption coefficient). A mode-locked Nd:YAG laser (Quantronix 416, $\lambda_0 = 1064$ nm) that pumps an amplifier (Continuum RGA 60-20) with a pulse duration of 100 ps, a repetition rate of 20 Hz, and pulse energies between 3 and 150 μJ were used. A lens (focal length of 120 mm) focused the beam to a minimum waist w_0 of around 20 μm. All measurements were referenced against a 1 mm thick cell filled with CS_2 ($n_2 = 3.2 \times 10^{-5}$ cm^2/GW) [13]. As expected no two-photon absorption was observed at $\lambda_0 = 1064$ nm for both $KNbO_3$ and $KTaO_3$.

The direct $\chi^{(3)}$ contribution to n_2 of $KNbO_3$ was determined from measurements on $KTaO_3$. Both materials are ferroelectric perovskite (ABO_3) compounds. Whereas $KTaO_3$ has cubic symmetry at room temperature, $KNbO_3$ is cubic only at high temperatures and transforms with decreasing temperature through the tetragonal phase to the orthorhombic phase at room temperature [14]. Here we assume that the contribution to n_2 arising from $\chi^{(3)}$ is the same for $KTaO_3$ and $KNbO_3$ [15]. In the cubic point group $m3m$ (assuming Kleinman symmetry [16]) there are only two independent tensor elements of $\chi^{(3)}$. We measured n_2 of $KTaO_3$ for light propagation along the crystallographic b direction both for light polarized along the crystallographic a axis as well as at 45° to this direction. From the measured values of $+(7.7 \pm 1.5) \times 10^{-6}$ cm^2/GW (proportional to $\chi_{1111}^{(3)}$) and $+(5.8 \pm 1.2) \times 10^{-6}$ cm^2/GW [proportional to $1/2(\chi_{1111}^{(3)} + 3\chi_{1133}^{(3)})$] we get $\chi_{1111}^{(3)} = +(1.3 \pm 0.3) \times 10^{-20}$ m^2/V^2 and $\chi_{1133}^{(3)} = +(2.2 \pm 0.4) \times 10^{-21}$ m^2/V^2 taking $n(KTaO_3) = 2.2$.

TABLE I. Comparison between theory and experiment for measurements along the main axis of the indicatrix and for propagation along $\theta = 45°$ off the c axis. The uncertainty of the theoretical as well as the measured values is 20%. n_2 is given in units of 10^{-6} cm^2/GW.

Propagation direction	Polarization	Direct $\chi^{(3)}$ n_2^{direct}	Cascading n_2^{SHG}	Cascading n_2^{OR}	Theory n_2	Experiment n_2
b	a	5.8	5.4	1.9	13	7.8
c	a	5.8	–	1.9	7.7	4.5
a	b	7.7	2.1	0.3	10	11
c	b	7.7	–	0.3	8	9.0
a/b	c	5.8	–3.4	4.4	6.8	5.6
45°	b-c plane	5.3	–2.6	19	22	26

The nonlinear refractive indices of $KNbO_3$ in the orthorhombic phase arising from direct $\chi^{(3)}$ processes can then be calculated from a rotation of 45° of the $\chi^{(3)}$ tensor around the b axis (Table I) [15]. Note that it is not possible to measure n_2^{direct} in $KNbO_3$ at room temperature since at least a contribution from n_2^{OR} always exists.

Experiments with $KNbO_3$ were performed with platelets cut normal to the crystallographic a, b, and c axes. In order to measure the largest contribution to n_2^{OR} arising from r_{232}, several propagation directions in the b-c plane were selected and platelets cut at 37.5°, 45°, and 71.4° with respect to the crystallographic c axis were prepared. Figure 2 shows an example of a Z-scan curve for $KNbO_3$ from which the positive sign of n_2 can be deduced immediately [13]. For light propagating along the c direction second-harmonic generation does not contribute to n_2 since the resulting polarization $P^{2\omega}$ is parallel to the propagation direction of the beam. For all other geometries this contribution has to be taken into account. Table I summarizes Z-scan measurements for light propagation and polarization along dielectric main axes of the crystals together with theoretical predictions. The values for the refractive indices and the nonlinear optical coefficients used for the calculation in Table I were taken from Refs. [17] and [18]. For our 100 ps pulses the electro-optic response of the bound electrons and optical phonons shows up instantaneously, whereas the elasto-optic contribution is clamped. Therefore the strain-free electro-optic coefficients and dielectric constants were used in the analysis of n_2^{OR} [19]. We see that the correspondence between theory and experiment is remarkably good for b- and c-polarized light. The discrepancy between theory and experiment for a-polarized light could possibly be attributed to a failure of our simple assumption that $\chi^{(3)}$ is exactly the same for $KTaO_3$ and $KNbO_3$.

The largest clamped electro-optic coefficient in $KNbO_3$ is $r_{232}^{s} = 360 \pm 30$ pm/V which can contribute to n_2 for light propagation as well as polarization within the b-c plane. In this plane we expect the largest value of n_2^{OR}; therefore we measured the nonlinear refractive index for several propagation directions, namely 37.5°, 45°, and 71.4° off the crystallographic c axis. Figure 3 shows the theoretically expected angular dependence of the different contributions to n_2 in $KNbO_3$. n_2^{direct} is almost constant over the whole angular range. n_2^{SHG} is always negative for the configuration in Fig. 3 and is approximately

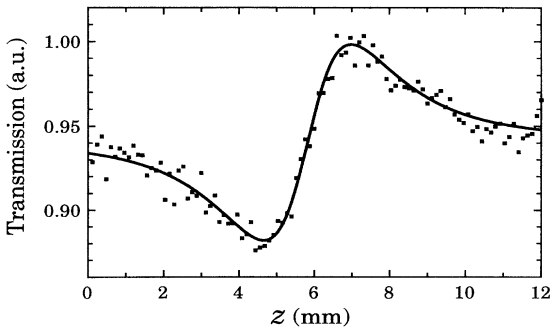

FIG. 2. Example of a Z-scan curve for a $KNbO_3$ plate (thickness $L = 0.976$ mm), cut normal to the crystallographic a axis, at $\lambda_0 = 1064$ nm. An intensity in the focus of $I_0 = 6.2$ GW/cm^2 (beam waist $w_0 = 22$ μm) was used in this example. A theoretical curve from the Z-scan analysis is also shown.

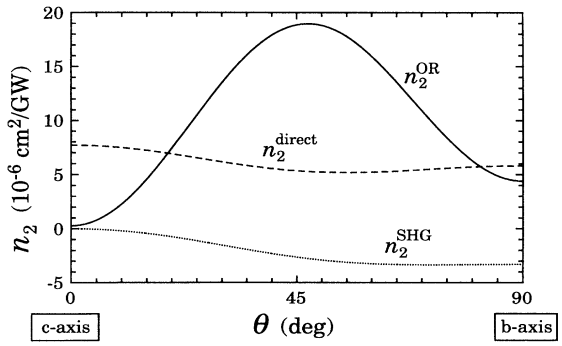

FIG. 3. Angular dependence of the different contributions to the nonlinear refractive index of $KNbO_3$ in the b-c plane. θ is the internal angle of propagation measured from the crystallographic c axis. The beam is polarized in the b-c plane as well. n_2^{direct} is almost constant over the whole angular range. n_2^{SHG} is always negative for the configuration shown here and is approximately constant. In contrast, the third term, n_2^{OR}, shows a pronounced angle dependence with a maximum value of 1.9×10^{-5} cm^2/GW at around $\theta = 47°$.

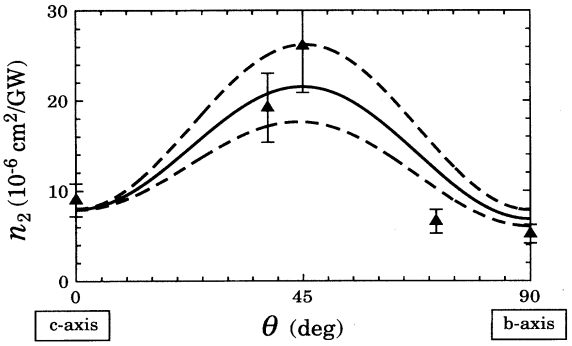

FIG. 4. Comparison of experimental and theoretical results of the nonlinear refractive index n_2 for $KNbO_3$ as a function of propagation direction in the b-c plane with in-plane polarized beams. The theoretical curves contain all three contributions to the nonlinear refractive index. The dashed curves are lower and upper limits mainly determined by the uncertainties of the electro-optic coefficients and dielectric constants.

constant. In contrast, the third term, n_2^{OR}, shows a pronounced angle dependence with a maximum value at around $\theta = 47°$.

Figure 4 shows the experimental results as well as the theoretical curve for all contributions. As expected a strong increase in the nonlinear refractive index is observed for the internal angles of incidence of 37.5° and 45°, where the contribution from r_{232}^s is more pronounced. The observed dependence of n_2 on the propagation direction and the increase in n_2 of more than a factor of three for an angle of $\theta = 47°$ can be explained only if the new cascaded second-order effects due to optical rectification and the linear electro-optic effect are considered.

In conclusion we have shown that there exists a large contribution to the nonlinear refractive index n_2 because of combined processes of optical rectification and the linear electro-optic effect. This contribution, which has been overlooked up to now, is always phase matched since all interacting waves either have the same optical frequency or have frequency zero. Another advantage of this new contribution to n_2 is that there is no net attenuation of the incident beam, in contrast to the contribution n_2^{SHG} where the fundamental is depleted [7]. It is also interesting to note that n_2^{OR} is always positive, also in contrast to n_2^{SHG} which can have either sign depending on the sign of the phase mismatch. Moreover, n_2^{OR} can also be present for light propagation along the polar axis. In such a case the longitudinal electro-optic effect becomes active. The fact that n_2^{OR} is always present in noncentrosymmetric materials also means that the measurements of the anistropy of n_2 in KTP, for example, should be reevaluated [10]. For a general propagation direction in a noncentrosymmetric material both n_2^{SHG} and n_2^{OR} are important for induced nonlinear phase shifts. It is, however, possible to find special orientations where one contribution is dominant as was shown here for $KNbO_3$.

[1] G. I. Stegeman and A. Miller, in *Photonics in Switching, Vol. I, Background and Components,* edited by J. E. Midwinter (Academic Press, Inc., Boston, 1993), p. 81.
[2] J.-M. R. Thomas and J.-P. E. Taran, Opt. Commun. **4**, 329 (1972).
[3] S. A. Akhmanov, A. I. Kovrygin, and A. P. Sukhorukov, in *Quantum Electronics: A Treatise,* edited by H. Rabin and C. L. Tang (Acadmic Press, New York, 1975), Vol. 1, Part B, p. 476.
[4] B. Wedding and D. Jäger, Appl. Phys. Lett. **41**, 1028 (1982).
[5] G. I. Stegeman, M. Sheik-Bahae, E. Van Stryland, and G. Assanto, Opt. Lett. **18**, 13 (1993).
[6] G. Assanto, G. Stegeman, M. Sheik-Bahae, and E. Van Stryland, Appl. Phys. Lett. **62**, 1323 (1993).
[7] M. L. Sundheimer, Ch. Bosshard, E. W. Van Stryland, G. I. Stegeman, and J. D. Bierlein, Opt. Lett. **18**, 1397 (1993).
[8] D. Y. Kim, W. E. Torruellas, J. Kang, Ch. Bosshard, G. I. Stegeman, P. Vidakovic, J. Zyss, W. E. Moerner, R. Twieg, and G. Bjorklund, Opt. Lett. **19**, 868 (1994).
[9] M. Zgonik and P. Günter, Ferroelectrics **126**, 33 (1992).
[10] T. K. Gustafson, J.-P. E. Taran, P. L. Kelley, and R. Y. Chiao, Opt. Commun. **2**, 17 (1970).
[11] R. DeSalvo, D. J. Hagan, M. Sheik-Bahae, G. Stegeman, E. W. Van Stryland, and H. Vanherzeele, Opt. Lett. **17**, 28 (1992).
[12] M. Bass, P. A. Franken, J. F. Ward, and G. Weinreich, Phys. Rev. Lett. **9**, 446 (1962).
[13] M. Sheik-Bahae, A. A. Said, W. Tai-Huei, D. J. Hagan, and E. W. Van Stryland, IEEE J. Quantum Electron. **26**, 760 (1990).
[14] G. Shirane, H. Danner, A. Pavlovic, and R. Pepinsky, Phys. Rev. **93**, 672 (1954).
[15] S. H. Wemple and M. DiDomenico, Jr., in *Advances in Materials and Device Research,* edited by R. Wolfe, Applied Solid State Science Vol. 3 (Academic, New York, 1972), p. 263.
[16] D. A. Kleinman, Phys. Rev. **126**, 1977 (1962).
[17] J.-C. Baumert, J. Hoffnagle, and P. Günter, in *Proceedings of ECOOSA,* Amsterdam, 1984 (SPIE, Bellingham, 1985); B. Bolger and H. A. Ferwerda, SPIE **492**, 374 (1985).
[18] B. Zysset, I. Biaggio, and P. Günter, J. Opt. Soc. Am. B **19**, 380 (1992).
[19] M. Zgonik, R. Schlesser, I. Biaggio, E. Voit, J. Tscherry, and P. Günter, J. Appl. Phys. **74**, 1287 (1993).